A Statistical Model of Cloud Vertical Structure Based on Reconciling Cloud Layer Amounts Inferred from Satellites and Radiosonde Humidity Profiles

WILLIAM B. ROSSOW

NASA Goddard Institute for Space Studies, New York, New York

YUANCHONG ZHANG

Department of Applied Physics and Applied Mathematics, and NASA Goddard Institute for Space Studies, Columbia University, New York, New York

JUNHONG WANG

National Center for Atmospheric Research, Boulder, Colorado

(Manuscript received 7 June 2004, in final form 9 December 2004)

ABSTRACT

To diagnose how cloud processes feed back on weather- and climate-scale variations of the atmosphere requires determining the changes that clouds produce in the atmospheric diabatic heating by radiation and precipitation at the same scales of variation. In particular, not only the magnitude of these changes must be quantified but also their correlation with atmospheric temperature variations; hence, the space–time resolution of the cloud perturbations must be sufficient to account for the majority of these variations. Although extensive new global cloud and radiative flux datasets have recently become available, the vertical profiles of clouds and consequent radiative flux divergence have not been systematically measured covering weather-scale variations from about 100 km, 3 h up to climate-scale variations of 10 000 km, decadal inclusive. By combining the statistics of cloud layer occurrence from the International Satellite Cloud Climatology Project (ISCCP) and an analysis of radiosonde humidity profiles, a statistical model has been developed that associates each cloud type, recognizable from satellite measurements, with a particular cloud vertical structure. Application of this model to the ISCCP cloud layer amounts produces estimates of low-level cloud amounts and average cloud-base pressures that are quantitatively closer to observations based on surface weather observations, capturing the variations with latitude and season and land and ocean (results are less good in the polar regions). The main advantage of this statistical model is that the correlations of cloud vertical structure with meteorology are qualitatively similar to "classical" information relating cloud properties to weather. These results can be evaluated and improved with the advent of satellites that can directly probe cloud vertical structures over the globe, providing statistics with changing meteorological conditions.

1. Introduction

Since most clouds in the earth's atmosphere are produced by upward air motions, the vertical distribution and microphysics (phase, particle size, and shape distributions) of cloud water mass are direct indicators of the presence and strength of these motions. The nature of the air motions also determines the morphological properties of the clouds: stronger, smaller horizontal-scale convective motions produce cumuloform clouds, whereas weaker, larger horizontal-scale synoptic motions produce stratiform clouds. However, this categorization is not always so simple; for example, marine stratus appear to be sustained by a balance between boundary layer turbulent (convective) motions and the large-scale circulation (e.g., Rozendaal and Rossow 2003). The feedback by clouds on the atmospheric motions that produce them is determined by the vertical and horizontal gradients of diabatic heating by both the precipitation formed in clouds and the radiative flux perturbations produced by the clouds (e.g., Rind and

Corresponding author address: William B. Rossow, NASA Goddard Institute for Space Studies, 2880 Broadway, New York, NY 10025.
E-mail: wrossow@giss.nasa.gov

Rossow 1984; Wang and Rossow 1998). The diabatic heating by radiation is proportional to the vertical gradients in radiative fluxes (flux divergence), which depend on the cloud type and vertical structure (e.g., Chen et al. 2000a,b). So the key to understanding cloud–dynamical feedback is determining the nature of the relations of radiative and latent heating rate profiles, induced by cloud vertical structure, to the atmospheric circulation. As one step toward this goal, we extend our studies of cloud effects on top-of-atmosphere and surface radiative fluxes (Rossow and Lacis 1990; Zhang et al. 1995; Rossow and Zhang 1995) to the determination of cloud effects on radiative heating rate profiles in the atmosphere (Zhang et al. 2004) for which we need information about cloud vertical structure. This paper describes our construction of a statistical model of cloud vertical structure (CVS) that is used for the calculation of radiative flux profiles (Zhang et al. 2004), but it also sets the stage for the study of the relation of CVS, itself, to meteorological conditions.

The two most extensive cloud datasets are those obtained from surface weather observations (SOBS) (Warren et al. 1986, 1988; Hahn et al. 1994, 1996) and weather satellites by the International Satellite Cloud Climatology Project (ISCCP) (Rossow and Schiffer 1991, 1999). The SOBS dataset provides information about the vertical distribution of cloud-base heights above local topography and the coincident occurrence, within a region about 30–50 km across, of clouds at different levels (Hahn et al. 1982, 1984, 2001; Warren et al. 1985). However, this information is not globally complete, coverage being particularly poor over the Southern Hemisphere oceans. The SOBS climatology (Warren et al. 1986, 1988) reports monthly mean and long-term-average results, but does not provide information about synoptic variations. The cloud-base vertical distributions reported in the climatology have been adjusted for the "bottom up" viewpoint using the collected coincident occurrence statistics and assuming a "random" overlap of cloud layers. Unadjusted vertical distribution information can be obtained from the processed individual observation dataset (Hahn et al. 1994, 1996), which can also be used to study diurnal-to-synoptic variations but only over those land areas where the sampling is sufficient. The surface observer only sees clouds at different levels in different parts of the sky; effectively the observer only sees the lowermost cloud base in each vertical column. Hence, direct information about cloud vertical structure is limited by the obscured, bottom-up view, so inferences about actual cloud vertical structure require making (statistical) assumptions that have yet to be verified. Nevertheless, the SOBS dataset, despite some well-documented limitations (discussed in the next section), provides the best view and most complete information available about the amount of low-level clouds.

The ISCCP dataset (Rossow and Schiffer 1999), which is globally complete and resolves mesoscale and synoptic-scale cloud variations, provides information about the vertical distribution of cloud-top pressures, which is equivalent to top heights above mean sea level, and the coincident occurrence, within a region about 280 km across, of clouds at different levels. The weather satellites also only see clouds at different levels in different parts of the sky; effectively the satellite only sees the uppermost cloud top in each vertical column. Hence, direct information about cloud vertical structure is limited by the obscured, top-down view, so inferences about actual cloud vertical structure require making (statistical) assumptions that have yet to be verified. Nevertheless, despite some well-documented limitations (discussed in the next section), satellites provide the best view and most complete information available about high-level clouds.

Some additional, but not complete, information on cloud vertical structure has been obtained from satellites using observations at more wavelengths than the two employed by ISCCP (e.g., Baum et al. 1994; Jin and Rossow 1997; Sheu et al. 1997; Lin et al. 1998) or by using different viewing geometries, such as limb scanning by the Stratospheric Aerosol and Gas Experiment (SAGE) instrument (Liao et al. 1995a,b; Wang et al. 1996; Wylie and Wang 1997). A more promising approach uses active sensors, such as lidars (Sassen 1991; Platt et al. 1994) and cloud radars (Kropfli et al. 1995) or both (Uttal et al. 1995; Wang et al. 1999) to profile cloud layers from the surface; however, these instruments cannot provide coverage of whole synoptic systems or complete global coverage until they are deployed on satellites (Stephens et al. 2002).

The coincident cloud layer occurrence statistics of Warren et al. (1985) and a study by Tian and Curry (1989) have been widely interpreted to suggest that simple statistical layer overlap relationships exist among layer cloud amounts, involving combinations of random and maximum layer overlap. This interpretation appears to have been strengthened by statistics from a ground-based cloud radar (Hogan and Illingworth 2000, 2003), but the latter studies tested no other possibilities than random overlap, maximum overlap, and a linear mixture of the two. Most importantly, they did not investigate whether their CVS observations showed any patterns associated with specific meteorological situations. Some authors have explored the utility of such simple layer overlap assumptions for

calculating radiative fluxes (see Chen et al. 2000b and references therein), finding that they do not work very well. If such simple statistical relations were really true, then it should be possible to infer the statistical CVS by combining the time-averaged SOBS and ISCCP datasets with some simple assumptions about these overlap statistics. Such an attempt was made by Weare (1999) but his results are flawed, as discussed in section 3b.

Actually, the Warren et al. (1985) results do not imply truly random occurrences of different cloud types but specific combinations of cloud types associated with specific meteorological situations (remember that the cloud types, themselves, indicate specific meteorology). This conclusion was reinforced by the study of Hahn et al. (2001), which showed that identification of specific morphological cloud types was more closely associated with characteristic mixtures of cloud types as seen from satellites. Warren et al. find that the strongest association is cirrus appearing with altostratus, especially over oceans; the Hahn et al. composites of ISCCP cloud types based on the surface observer's classification of types present, show a similar association of cirrus with middle-level clouds. However, the Hahn et al. results also suggest that this might be an association between thinner and thicker high-level clouds in SOBS and/or some misclassification by ISCCP of cirrus plus low-level clouds as middle-level clouds. That the next most common association is cirrus with low-level clouds is of particular note in this study because the satellite observations have the most trouble correctly identifying this type (cf. Jin and Rossow 1997). Similarly, Lau and Crane (1995, 1997) show that specific combinations of cloud types, whether observed from satellites or the surface, occur within particular meteorological situations. In other words, the relationships of cloud types and/or cloud vertical distribution are a structured, not random, characteristic of the meteorology—hence the long-standing practice of making cloud observations in support of weather forecasts. Simple cloud-layer overlap statistics do not capture this meteorology-dependent CVS.

Radiosonde measurements (raobs) of the vertical profiles of temperature and humidity as they penetrate cloud layers provide direct information about cloud vertical structure by identifying saturated levels in the atmosphere; however, raobs coverage of the globe is even sparser than SOBS. Wang et al. (2000) report zonal mean (separately for land and ocean) statistics of cloud layers from an analysis of a 20-yr (1976–95) collection of twice-daily radiosonde data from all available surface sites. This climatology is too sparse to resolve the mesoscale to synoptic-scale variations of CVS. Nevertheless, the raobs dataset, despite some well-documented limitations (discussed in the next section), provides the only direct and complete information about middle-level clouds, especially those that co-occur with other clouds at other levels. The main results from Wang et al. (2000) are: 1) somewhat more than half of all clouds are single layered and only a few percent exhibit more than three layers; 2) the distribution of cloud layer thicknesses exhibits a modal value of about 500 m, with a secondary mode at about 6 km: the average value is about 1.5 km; 3) multilayered clouds generally include a low-level cloud layer; and 4) there are two distinct populations of cloud layers, the majority with a very nearly constant distribution of layer thicknesses independent of height and the minority with layer thicknesses that increase monotonically with cloud-top height.

To calculate global radiative flux profiles that resolve weather-scale variations, we need to combine these incomplete sources of information into a statistical model of cloud vertical structure because we do not have any single CVS dataset with the needed space–time resolution. Moreover, since there is strong evidence that CVS is related to the meteorology like cloud types are and, as we discuss in the next section, the limitations of each of these datasets are also dependent on meteorological conditions, we need a statistical model that goes beyond combining the time-averaged statistics to one that provides CVS that is related to the satellite-observed cloud types. By comparing the layer cloud amounts observed from ISCCP and raobs, we have identified such relationships between the cloud types that can be recognized from satellites and specific vertical structures: we use these relationships to augment the ISCCP cloud property information (fractional cover, top location, and optical thickness) with information about cloud layer thickness and the occurrence of hidden lower-level cloud layers to determine cloud-base locations. The resulting statistical model relates the ISCCP-observed cloud properties to the raobs-observed cloud vertical structure as a function of season and latitude, separately over ocean and land.

After describing the raobs and ISCCP datasets, along with the SOBS dataset used to verify low-level cloud amounts, and their most salient limitations (section 2), we highlight the key relationships between the original vertical distributions of cloud tops from these datasets and explore simple hypotheses to reconcile them (section 3). We then compare the low-level cloud amounts derived from these statistical models of cloud vertical structure to the low-level cloud amounts directly observed from SOBS as a limited, but the only available, form of verification. In section 4 we describe the com-

plete 3D CVS model, produced by combining the raobs and ISCCP statistics (the complete digital dataset will be released publicly). Finally, in section 5 we discuss some of the implications of the results.

2. Datasets

The results shown in this paper are based on monthly statistics obtained from geographically matched, individual observations covering the period from 1990 to 1992. This limited period was chosen to coincide with the period covered by several other climatological datasets used in the development and testing of the revised radiative flux analysis (cf. Rossow and Zhang 1995; Zhang et al. 2004). In particular, we matched individual observations from three systems: raobs, ISCCP, and SOBS; the availability at the time of the study several years ago of the individual observations from the latter source limited the choice of time period. Although the effects of the Mt. Pinatubo volcanic eruption on the ISCCP results (Rossow and Schiffer 1999; Luo et al. 2002) cause a several percent decrease (increase) in cirrus (cumulus) cloud amounts at maximum, the effect on the 3-yr-average statistics is $<1\%$. Since the interannual variability of cloud types in specific geographic regions is smaller than their synoptic and seasonal variability, three years of statistics are sufficient for the comparison.

a. Cloud vertical structure climatology from radiosonde humidity profiles

Radiosondes are launched by world weather services twice daily at most stations to measure vertical profiles of temperature, humidity, and winds. Although there are many hundreds of launch sites scattered around the world, they are concentrated in Northern Hemisphere land areas and provide much less information about the atmosphere over oceans, especially in the Southern Hemisphere. Much has been written about the accuracy and usefulness of these data for studying the atmosphere and climate (temperature, humidity) variations (see references in Ross and Elliott 2001; Seidel et al. 2004). Under the assumption that cloud layers will have relative humidities near 100%, Poore et al. (1995) developed a simple analysis method to identify saturated (cloud) layers in the radiosonde humidity profiles. This methodology was extended and generalized by Wang and Rossow (1995) and used to produce a 20-yr climatology of cloud layer structure (Wang et al. 2000), which we will call the raobs dataset (available from the authors). Because of the sparse geographic coverage, they reported only zonal mean results, although separated into land and ocean areas. The cloud vertical structure in the raobs climatology is described in terms of the vertical distributions of cloud-base and cloud-top heights above mean sea level, cloud layer thicknesses and separation distances, and the co-occurrence of cloud layers at different levels. The quantity, "layer cloud amount" for this dataset is a frequency of occurrence.

For this study we use the individual profiles for the 1990–92 period that are matched geographically with ISCCP and SOBS. For our use, we reclassify all of the raobs cases as follows: 1) first, each cloud is classified as high (H), middle (M), or low (L) depending on the cloud-top pressure for each separate layer, using the same pressure divisions that are used in the ISCCP cloud dataset (680 mb separates low-level and middle-level clouds and 440 mb separates middle-level and high-level clouds); 2) second, separate cloud layers occurring in the same height category (H, M, L) are combined into a single cloud layer defined by the uppermost top and lowermost bottom (based on the statistics in Wang et al. 2000, this affects only about 3%–5% of the cases); and 3) third, each case is further classified by the whole cloud vertical structure as single-layer clouds (called 1H, 1M, 1L), double-layer clouds (HL, HM, ML), and triple-layer clouds (HML). By definition,

$$\mathrm{H} = 1\mathrm{H} + \mathrm{HL} + \mathrm{HM} + \mathrm{HML}, \tag{1a}$$

$$\mathrm{M} = 1\mathrm{M} + \mathrm{ML} + \mathrm{HM} + \mathrm{HML}, \tag{1b}$$

$$\mathrm{L} = 1\mathrm{L} + \mathrm{ML} + \mathrm{HL} + \mathrm{HML}, \tag{1c}$$

where H, M, and L refer to the total amount of clouds at each level regardless of whether other cloud layers are present.

As Wang et al. (2000) discuss, there are some limitations of the raobs results that are important for our study. The two most notable concern errors in the cloud-base location in moist marine boundary layers, which causes an overestimate of low cloud amount over oceans by about 10% (see also Wang et al. 1999), and missed high-level cirrus clouds, particularly when thin, scattered cirrus are predominant, which causes an underestimate of high cloud amount by about 5%–10%. The latter problem was associated with the poor performance of the humidity sensors at cold temperatures (Wang et al. 2002, 2003) and in the Tropics with the fact that the maximum altitude reached by most balloons is well below the tropopause (Wang and Rossow 1995). Another problem with the detection of ice phase clouds concerns the fact that the analysis of the radiosonde relative humidities identifies a cloud layer with a threshold value just below 100% (relative to ice at temperatures <273 K), so the tendency of ice clouds to

form at humidities significantly greater than 100% (Gierens et al. 1999; Spichtinger et al. 2003) means that our analysis of the humidity profiles may overdetect cloud layers in persistently cold regions. As we will see, the raobs results indicate much more upper-level cloudiness than is seen by the satellites in the polar regions and winter northern midlatitudes, which may be caused by this problem.

b. Cloud-top pressure distribution from ISCCP

The ISCCP dataset, based on satellite visible and infrared radiance observations, provides global coverage sampled at 3-h, 30-km intervals. The main cloud properties from the ISCCP D1 dataset (Rossow et al. 1996) are cloud areal coverage for regions about 280 km in size, cloud-top pressure, and optical thickness (we use daytime statistics only because the two-wavelength analysis provides a more accurate representation of cloud-top locations; cf. Rossow and Schiffer 1999). For the first part of this study, we focus on the height categories, referring to the ISCCP clouds as high (HI), middle (MI), and low (LI). Later, we subdivide each layer category into ranges of optical thickness (referred to as thin, medium, and thick). Since each satellite pixel (covering an area about 5 km in size on average, but sampled at 30-km intervals) is treated as cloudy or clear, the ISCCP areal cloud amounts, when normalized by the total cloud cover, are equivalent to a point-measurement frequency of occurrence like that reported in the raobs dataset. When we compare actual area cloud amounts from the satellite to area cloud amounts from surface observers, then this quantity can be considered to be the usual cloud fraction (Rossow et al. 1993).

A number of studies, summarized in Rossow and Schiffer (1999), have evaluated the accuracy of the ISCCP height assignments and cloud detections. The most notable biases, which are important for this study, are 1) a tendency to overestimate physical cloud-top pressures for high-level clouds by about 100 mb on average, especially at low latitudes (Liao et al. 1995b), which does not generally change their classification as high clouds; 2) an underdetection of isolated, very optically thin cirrus clouds, equivalent to cloud cover of about 10% (Liao et al. 1995a; Jin et al. 1996; Stubenrauch et al. 1999); and 3) the misclassification of multilayered clouds if the upper layer is optically thin, representing about 25% of the high cloud cases (cf. Jin and Rossow 1997; Stubenrauch et al. 1999). We also note that cloud detection in the polar regions is especially difficult because of the low radiometric contrasts encountered; this causes an underestimate of total cloud cover, particularly in summertime, associated with missed low-level clouds: The amount of this underestimate is hard to estimate because other available datasets are also uncertain (Rossow and Schiffer 1999).

c. Surface weather observations of cloud types

The surface weather observations (SOBS), which were also collected to support weather forecasting, include a visual classification by an observer of the clouds in terms of the amount and morphological type of clouds that can be converted into estimates of the cloud amounts at different levels (Warren et al. 1986, 1988; Hahn et al. 1982, 1984). We collect the SOBS cloud types into three height categories [low (LS), middle (MS), and high (HS)]. When normalized by the total cloud cover, these cloud amounts are also equivalent to the raobs frequencies of occurrence. We will also compare the absolute cloud fraction of low-level clouds from SOBS with the areal values reported by ISCCP, both the original values and the values modified by our new statistical models.

The SOBS dataset is collected at about ten times more sites than raobs, but they are still concentrated heavily in Northern Hemisphere land areas. Hahn et al. (2001) have examined the relationships between the SOBS and ISCCP cloud types, finding the best correspondence when combinations of clouds are classified by meteorological situation (cf. Lau and Crane 1995, 1997). In general, ISCCP and SOBS agree very well on the presence of low-level and the thicker middle-level clouds, when they are not obscured by upper-level clouds in the satellite view (Hahn et al. 2001). However, this comparison also reveals a little-known feature of the SOBS height classification: according to the WMO instructions for discriminating between middle and high clouds, this classification depends on their transparency to sunlight since there is no actual information on height. Thus, in the comparison with ISCCP, although there is a slight tendency for optically thinner clouds to be somewhat higher, the ISCCP cloud-top height distributions were almost the same for both the MS and HS cases. Hence, we use the SOBS dataset only as an independent verification of the reconstructed low cloud amounts (cf. Wang et al. 2000). The SOBS low cloud amount, LS is the sum of the cumulus, stratocumulus, and stratus cloud types (it also includes cumulonimbus, but these constitute only a few percent of the total).

d. Matching statistics

Because the raobs results are spatially very sparse, particularly in comparison to the satellite coverage, we use zonal mean statistics obtained from geographically matched observations for the comparisons of results

TABLE 1. Comparison of original raobs and ISCCP cloud layer amounts (%) normalized to a total cloud amount of unity. The raobs layer amounts are labeled by L, M, H, and the ISCCP layer amounts by LI, MI, HI; "-r" indicates amounts assuming random overlap; "-m" indicates amounts assuming maximum overlap, where LI-m = 100. The number of matched 2.5° grid cells in each latitude zone is indicated at the bottom of the table (ranging from 11% of the tropical zone's area to 55% of the midlatitude zone's area).

	Land				Ocean			
Cloud layer	15°S–15°N	15°–35°N	35°–65°N	65°–90°N	15°S–15°N	15°–35°N	35°–65°N	65°–90°N
L	68	52	49	56	82	81	79	73
1L	26	31	22	20	47	52	40	31
LI	21	24	21	26	37	43	40	40
LI-r	39	40	43	53	59	66	68	69
M	44	32	32	31	27	22	29	36
MI	27	30	40	48	23	24	34	47
MI-r	50	50	59	62	42	40	49	54
MI-m	79	76	79	74	63	57	60	60
H	50	47	57	59	39	34	42	43
HI	52	46	39	25	40	33	26	13
No. of cells	32	137	307	17	152	203	298	39

and to develop the statistical models that reconcile the results. To form these statistics we first geographically match 3-yr mean monthly values from raobs with ISCCP (and SOBS for verification) on the ISCCP equal-area grid with a grid resolution of 2.5° at the equator and then calculate zonal means (separately for ocean and land). Missing latitudes (2.5° intervals) are filled by a three-step process: 1) each missing latitude zone is filled by the average over seven zones centered on the target zone (smoothing); 2) any zones still without values are filled by replication from the nearest zone within ±5°; and 3) any zones still without values are filled by replication from the nearest month (same zone) that has values within ±3 months (seasonal smoothing). These zonal mean results are compared directly and the statistical models are based on these statistics; however, when this information is summarized in the tables and figures, larger zones are produced by combining these 2.5° statistics.

3. Hypotheses for reconciling the observations

a. Original layer cloud amounts

Table 1 shows the annual average amounts of low, middle, high clouds, normalized by total cloud amount, originally reported by raobs (L, M, H) and ISCCP (LI, MI, HI) for four latitude zones separated into land and water. The data included in each zonal average are only those from grid cells in the ISCCP equal-area map that contain both raobs and ISCCP (as well as SOBS) observations. The number of cells for each zone is indicated; this represents an area sampling fraction ranging from 11% of the tropical zone to 55% of the midlatitude zone. We normalize each dataset's layer cloud amounts to its total cloud amount to make the observations equivalent and to minimize any effects of differing cloud detections (for convenience "layer amount" will generally be used to refer to these normalized values; the word "absolute" will be added to indicate the real layer cloud fractions). The raobs results report clouds at all levels, even when overlapped; hence, the sum of the three layer amounts can exceed 100%. Table 1 also shows the isolated low clouds (1L) detected by raobs. The ISCCP results report only those cloud levels seen from above (no overlap), so the normalized layer amounts sum to 100%. Two other versions of the ISCCP results are shown to illustrate the effects of applying the simple random and maximum layer overlap assumptions.

If both raobs and ISCCP were perfect measurements and the top-down viewpoint of the satellite were the only factor causing differences, then the following relationships would be true by definition (see section 2 for definitions of symbols):

$$\mathrm{HI} = \mathrm{H} = 1\mathrm{H} + \mathrm{HL} + \mathrm{HM} + \mathrm{HML}, \quad (2a)$$

$$\mathrm{MI} = 1\mathrm{M} + \mathrm{ML}, \quad (2b)$$

$$\mathrm{LI} = 1\mathrm{L} \quad (2c)$$

(remember that the quantities on the right-hand side are the true layer cloud amounts from raobs). In other words, the effect of the satellite viewpoint causes, comparing (1) and (2), HI = H, MI < M, and LI ≪ L.

Table 1 shows that HI ≈ H at lower latitudes, but at higher latitudes HI < H. Both of these results are unexpected because comparison of raobs high-level cloud

TABLE 2. Raobs climatology of cloud layer combinations.

	Land				Ocean			
Layer type	15°–15°N	15°–35°N	35°–65°N	65°–90°N	15°S–15°N	15°–35°N	35°–65°N	65°–90°N
1L	26	31	22	20	47	52	40	31
1M	14	16	14	13	5	6	7	11
ML	11	5	7	8	10	8	10	14
1H	13	26	30	26	10	10	11	13
HL	18	11	15	23	17	15	20	20
HM	6	6	7	5	3	3	3	3
HML	13	4	4	5	9	6	8	7
L	68	51	48	56	83	81	78	72
M	44	31	32	31	27	23	28	35
H	50	47	56	59	39	34	42	43

amounts with lidar observations showed that raobs miss high-level clouds in the Tropics because of the limited altitudes reached by the balloons and miss the thinner, more scattered cirrus types at midlatitudes (Wang et al. 2000). Although the ISCCP measurements also miss the very thinnest cirrus (Liao et al. 1995a; Jin et al. 1996; Stubenrauch et al. 1999), the satellite sensitivity to thin cirrus is greater than that of raobs, so we would have expected HI $>$ H.

The ISCCP treatment of high-level clouds with low optical thicknesses is probably about right since there cannot be much cloud below them; otherwise the optical thickness would be much larger (however, see Chen and Rossow 2002). The main problem for the ISCCP analysis is the misclassification of cloud-top height when cirrus overlie lower-level clouds (Jin and Rossow 1997); the most significant case is when cirrus overlie low-level clouds, which would look like a middle-level cloud with moderate optical thicknesses. The raobs climatology (Table 2) shows that for double-layer clouds the lowermost cloud is most often a low-level cloud (Wang et al. 2000). The SOBS climatology also shows a clear association of cirrus and boundary layer cloud types (Warren et al. 1985). Jin and Rossow (1997) conclude that cirrus occur over lower-level clouds about 25% of the time (relative to all high clouds), which is similar to the relative amount of HL found in the raobs climatology (Table 2). Thus, the general agreement of H and HI at lower latitudes appears to be a fortuitous cancellation of underestimates by both raobs and ISCCP.

The situation at higher latitudes is more difficult to interpret: the several comparisons of ISCCP to other satellite measurements suggest that, if anything, the ISCCP underestimate of high-level clouds should be smaller than at lower latitudes (cf. Liao et al. 1995a,b). On the other hand, the humidity sensor on the weather balloons is operating at very low temperatures, particularly in the polar regions, which causes significant response delays that grow longer at lower temperatures. In situations just below freezing temperatures, the sensor can also ice up, causing reports of saturation (or greater) at levels above the actual cloud top. These effects would both cause overestimates of cloud layer thicknesses and upper-level cloudiness. Wang et al. (2000) report cloud layer thicknesses $>$200 mb at 50°N in wintertime that may result from this problem. Naud et al. (2003) used the cloud radar/lidar at the Atmospheric Radiation Measurement (ARM) Southern Great Plains (SGP) site to assess the Wang and Rossow (1995) and Chernykh and Eskridge (1996) radiosonde analysis methods and found that both report higher cloud tops than do the active sensors. The discrepancy shown in Table 1, which also appears at midlatitudes in wintertime but not summertime, might also be exaggerated by a tendency for ice phase clouds to form less readily at relative humidities near 100%. If significant amounts of high-level clouds at higher latitudes form at relative humidities greater than 100%, then our analysis of raobs will overestimate the frequency of clouds at such low temperatures, reinforcing the other problems just discussed. For example, in the upper atmosphere, the average supersaturation in air with relative humidities $>$100% is 15%, about half that needed for homogeneous nucleation of ice (Gierens et al. 1999; Spichtinger et al. 2003); if roughly similar conditions prevail at lower altitudes and at somewhat warmer temperatures, then the raobs cloud amounts will be overestimates, explaining the fact that HI $<$ H.

If raobs and ISCCP were perfect, then one would expect MI $<$ M, but this is only true in the Tropics, especially over land areas (Table 1). Given the tendency for ISCCP to misclassify cirrus overlying lower-level clouds, it may be that the excess middle-level

clouds in ISCCP more than compensate for the obscuration of middle-level clouds by high-level clouds.

As expected, LI << L by a factor of 2 or 3, despite some of the effects discussed above. This underestimate of low-level cloud amount in the ISCCP dataset was also reflected in the comparison of the average cloud-base pressures obtained from ISCCP and raobs (Zhang et al. 1995), which showed that the average ISCCP cloud-base pressure, based on assuming all clouds to be single layered with climatological layer thicknesses, was too low by about 50–100 mb at most latitudes, but by about 200–250 mb in the Tropics. Contrasting the synoptic composite distributions of layer cloud amounts found using satellite and surface cloud observations, Lau and Crane (1997) show specific disagreement in the frontal areas, where the satellite data show a predominance of high-level clouds and the surface observations show a predominance of low-level clouds and characteristic mixtures of high and low clouds ahead of and behind the cyclone. However, Table 1 shows that LI $\approx$ 1L, suggesting that the relative amount of isolated low cloud detected by ISCCP is about right. The small tendency for LI < 1L, particularly in lower latitudes over ocean, is consistent with a tendency of the raobs to miss some of the high, thin cirrus (increasing the relative amount of isolated low cloud) and to overestimate low-level clouds in moist boundary layers.

Table 2 shows the climatology of CVS from the raobs analysis (Wang et al. 2000), where the layer amounts are normalized to total cloud amount. Notable features are that 1) the 1H category, isolated thin cirrus, is about 10% of total high-level clouds over oceans but about 25%–30% over land, a difference also found by Warren et al. (1985); 2) the HL category, which may be misclassified by ISCCP as middle-level clouds, constitutes about 15%–20% of the total high-level clouds, consistent with the estimates by Warren et al. (1985) and Jin and Rossow (1997); 3) more than half of middle-level clouds co-occur with either high- or low-level clouds, again consistent with Warren et al. (1985); and 4) about half of the low-level clouds co-occur with upper-level clouds, consistent with Warren et al. (1985) and Hahn et al. (2001).

b. *Layer cloud amounts estimated using random or maximum overlap assumptions*

The two simplest hypotheses to reconcile the satellite viewpoint with the raobs profiles are that cloud layers overlap either maximally or randomly: The first hypothesis is that all possible levels below the observed level are always occupied by clouds, and the second hypothesis is that the probability of a cloud occurring in an obscured level is the same as cloud observed in unobscured areas. The original ISCCP results are equivalent to no overlap (if there are no misclassifications), the opposite extreme from maximum overlap. Table 1 shows the middle-level and low-level cloud amounts that would be inferred from ISCCP using these two simple hypotheses (the low-level cloud amount for maximum overlap is not shown since it is always 100% for the normalized amounts). In general, these simple assumptions do not improve the estimates: middle-level clouds are generally overestimated by both random and maximum overlap, whereas low-level clouds are still underestimated by random overlap and overestimated by maximum overlap. Since the raobs has a tendency to overestimate low clouds, particularly over oceans (Wang et al. 1999), the maximum overlap results are not really an improvement for low clouds. These simple results are consistent with other studies for low-level clouds that concluded that a mixture of random and maximum overlap was needed (Tian and Curry 1989; Hogan and Illingworth 2000, 2003); however, such a mixture cannot account for the middle-level clouds.

Weare (1999) proposed a more sophisticated merger approach for the ISCCP and SOBS monthly mean layer cloud amounts by finding the best compromise of the probabilities of occurrence of each CVS that reconciles the two observations. Although this is a good approach, there are flaws in this particular study that undermine its results.

First, the mathematical formulation ignores the fact that there are other reasons (e.g., detection sensitivity) for differences in layer cloud amount between the two datasets (as discussed above and more thoroughly in Rossow et al. 1993) so that combining these two datasets as if their total cloud amounts agreed exactly (which they do not) amounts to requiring the viewpoint difference to explain all differences. Use of unnormalized layer amounts leads to physical inconsistencies in some places where the results indicate that the top-down viewpoint sees more low-level cloud than the bottom-up viewpoint, contradicting the basic underlying assumption of the analysis. Weare (1999) concludes generally from his results that "the atmosphere has fewer low clouds and more middle and high clouds than is indicated by the ISCCP C2 observations," which does not make sense if the viewpoint is the only cause of disagreement between the two datasets.

Second, the method requires four assumptions: a first guess of the CVS probability distribution, its uncertainty, and the estimates of the uncertainties of the ISCCP and SOBS datasets. The uncertainties determine the weight given to the first guess and the two datasets. The choices that Weare (1999) makes give twice the weight to the first guess, which is that the CVS

is that seen by SOBS, than to the observations. However, since no citations or evidence in support of these choices is presented, the particular ones used must be considered ad hoc. In fact, the estimates of the observational uncertainties that Weare uses (20% rms) are not consistent with the literature. Rossow et al. (1993) find that monthly mean SOBS and ISCCP C2 agree to within 3%–5% rms, a much smaller difference than that assumed by Weare.

Finally, the results presented neglect the fact that the ISCCP classifies clouds by the location of their cloud tops above mean sea level whereas SOBS classifies clouds by the location of their cloud bases above the local topography. Even though the ISCCP layer definitions account approximately for this difference in terms of an average cloud layer thickness, the ISCCP cloud height categories over land are not the same as the SOBS categories, especially where there is any significant topography. Although this difference is noted by Weare (1999), there is no investigation of the quantitative effect on the results.

Random or maximum overlap does not work, a conclusion that Weare (1999) also supports. When considering monthly means, it may well be that the "mixed" overlap approach can work (Weare 1999) but, as Table 1 suggests, middle-level cloud amounts cannot be explained this way. All of the studies by Warren et al. (1985), Lau and Crane (1995, 1997), and Hahn et al. (2001) confirm the (obvious) point that the cloud vertical structure exhibits specific correlations that are dependent on the meteorological situation. We will also show some evidence here for a more deterministic relationship rather than the simple statistical ones.

c. *Model A*

Before looking for a cloud-type dependent relationship between the ISCCP and raobs cloud layer amounts, we explore the simplest hypothesis that can reconcile the raobs and ISCCP datasets (this model is a simple ad hoc adjustment of the datasets to reconcile them). Recall the salient features of the comparison in the previous section: 1) HI $\approx$ H at lower latitudes but HI $<$ H at higher latitudes instead of HI $>$ H at all latitudes; 2) MI $\approx$ M, implying that MI is larger than expected; 3) L $>>$ LI $\approx$1L, as expected; and 4) the relative amount of HL is similar to the estimated occurrence of cases where the ISCCP analysis underestimates cirrus cloud-top height because of the presence of an underlying cloud layer at low levels. Taken together these facts suggest that the raobs and ISCCP layer cloud amounts might be reconciled by assuming that 1) all HL clouds are misclassified by ISCCP as middle-level clouds and 2) raobs is missing some of the thin cirrus that should be in the 1H category. In other words [cf. Eq. (2)],

$$\mathrm{HI}' = 1\mathrm{H}^* + \mathrm{HM} + \mathrm{HML}, \tag{3a}$$

$$\mathrm{MI}' = 1\mathrm{M} + \mathrm{ML} + \mathrm{HL}, \tag{3b}$$

$$\mathrm{LI}' = 1\mathrm{L}, \tag{3c}$$

where the primed ISCCP cloud amounts are what is actually observed. Since HI′ is already in good agreement with H from raobs, at least in the Tropics, we must increase 1H to compensate for the increase of HI′ produced by adding back HL to this category. In the polar regions we use this correction to decrease the excessive raobs high cloud amounts. Thus,

$$1\mathrm{H}^* = 1\mathrm{H} + (\mathrm{HI}' + \mathrm{HL} - \mathrm{H}), \tag{4a}$$

$$\mathrm{H}^* = 1\mathrm{H}^* + \mathrm{HL} + \mathrm{HM} + \mathrm{HML}, \tag{4b}$$

where an asterisk indicates the corrected amount. Although we could take the value of HL directly from Table 2, the cirrus missed by raobs means that 1H is too small and HL too large in relative terms. Moreover, since the relationships among the layer cloud amounts are not exact, we choose to estimate HL as the average of the direct value with the two other values that can be obtained from (3b) and (1c); namely,

$$\mathrm{HL}_\mathrm{h} = \mathrm{HL}, \tag{5a}$$

$$\mathrm{HL}_\mathrm{m} = \mathrm{MI}' - (1\mathrm{M} + \mathrm{ML}), \tag{5b}$$

$$\mathrm{HL}_\mathrm{l} = \mathrm{L} - (\mathrm{ML} + \mathrm{HML}) - \mathrm{LI}, \tag{5c}$$

and

$$\mathrm{HL}^* = (\mathrm{HL}_\mathrm{h} + \mathrm{HL}_\mathrm{m} + \mathrm{HL}_\mathrm{l})/3. \tag{6}$$

With the adjustments to 1H and HL, which have simply been made to force agreement, the ISCCP layer cloud amounts can be corrected, using the raobs statistics, to obtain

$$\mathrm{HI}^* = \mathrm{HI}' + \mathrm{HL}^*, \tag{7a}$$

$$\mathrm{MI}^* = \mathrm{MI}' - \mathrm{HL}^* + \mathrm{HM} + \mathrm{HML}, \tag{7b}$$

$$\mathrm{LI}^* = \mathrm{LI}' + \mathrm{ML} + \mathrm{HML} + \mathrm{HL}^*, \tag{7c}$$

with the results shown in Table 3 as Model A. From a comparison of Tables 1 and 3 for different reconstructions of low-level and middle-level cloud amounts, asterisks are placed beside the numbers from the model that provides the most accurate result for each cloud level and latitude zone. The only cases for which random overlap is slightly superior to Model A are for low clouds over polar land and midlatitude oceans (indicated by a double asterisk); maximum overlap is closer to raobs than Model A for low clouds over oceans at lower latitudes, but is excessive (100% relative

TABLE 3. Comparison of original raobs and two statistical models based on ISCCP cloud layer amounts (%) normalized to a total cloud amount of unity. The raobs layer amounts are labeled by L, M, H, and the ISCCP layer amounts by LI, MI, HI; "-A" and "-B" indicate the two models; H* indicates the high cloud amounts after adjusting the raobs amount for underdetection. The asterisks by certain numbers in the table indicate the best match to the raobs layer amount among the four models (random, maximum, Model A, and Model B); a double asterisk indicates that random overlap produces just as good an estimate. A cross indicates that maximum overlap is a closer estimate, but it is always an overestimate of a value that is probably too large so that the model with a larger amount is the better of the two ISCCP-based models (always better than random overlap).

	Land				Ocean			
Cloud layer	15°S–15°N	15°–35°N	35°–65°N	65°–90°N	15°S–15°N	15°–35°N	35°–65°N	65°–90°N
L	68	52	49	56	82	81	79	73
LI	21	24	21	26	37	43	40	40
LI-A	*47	38	39	49	†61	†62	**69	*71
LI-B	42	*43	*44	**54	53	59	67	71
M	44	32	32	31	26	22	29	36
MI	27	30	40	48	23	24	34	47
MI*-A	*40	40	44	*45	*29	25	34	*44
MI*-B	28	*31	*41	48	22	*23	*32	46
H	50	47	57	59	39	34	42	43
H*	65	50	48	43	61	50	47	31
HI	52	46	39	25	40	33	26	13
HI*-A	59	51	50	40	46	40	38	26
HI*-B	63	54	49	35	47	39	35	21

amount). Since the raobs themselves are probably an overestimate in this region, the Model A (and B) results are actually to be preferred (as we show below by comparison with SOBS in section 3e).

d. Model B

Model A, although motivated by specific shortcomings of the two datasets, is based on monthly, zonal mean statistics (land and ocean separately) and provides only a correction to the cloud layer statistics; it cannot be applied to individual situations. Likewise, the results of Weare (1999) cannot be used for our purposes because they provide only the monthly mean statistics. For the studies described in the introduction, we need a model that specifies the cloud vertical structure for each cloud type identified from the satellite in order to produce CVS variations that are also correlated with the meteorology. That this approach can work is suggested by the findings of Lau and Crane (1995, 1997), which show that the ISCCP cloud types defined by cloud-top pressure and optical thickness appear in the expected locations within meteorological systems and are correlated with the classical cloud types from weather observers, by the findings of Hahn et al. (2001), which show that the classical and ISCCP-defined cloud types correspond especially when meteorologically significant combinations of clouds are considered to represent cloud system types, and by Jakob and Tselioudis (2003), who show that distinct meteorological states of the Tropics can be identified by specific patterns of the cloud-top pressure and optical thickness distributions (equivalent to specific mixtures of cloud types) obtained from ISCCP.

In Model B, we make the plausible assumption that increasing (total column) optical thickness corresponds to an increasing numbers of cloud layers: smaller optical thicknesses correspond to single-layer clouds, an intermediate range of optical thicknesses corresponds to double-layer clouds, and larger optical thicknesses correspond to three-layer clouds. This correspondence is consistent with Fig. 11 in Wang et al. (2000), which shows that the majority of clouds exhibit a roughly constant physical layer thickness distribution independent of top height. We also assume that lower-level layer clouds have somewhat larger optical thicknesses (larger water contents) than upper-level clouds for the same physical layer thickness. Wang et al.'s results also show a smaller population of clouds with layer thicknesses that increase linearly with increasing top height; we assume that these correspond to convective clouds and associate them with the largest optical thicknesses (cf. Fu et al. 1990; Machado and Rossow 1993; Machado et al. 1998). Using these assumptions and adjusting the optical thickness cutoffs, where needed, to provide the best agreement between ISCCP and raobs, we define high ISCCP clouds with $\tau < \tau_A$ to be single-layer clouds, those with $\tau_A < \tau < \tau_B$ to be double-layer clouds, those with $\tau_B < \tau < \tau_C$ to be three-layer clouds, and those with $\tau > \tau_C$ to be convective clouds that extend from near the surface to the observed cloud top.

TABLE 4. ISCCP climatology of cloud types (see Fig. 2 in Rossow and Schiffer 1999).

	Land				Ocean			
Cloud type	15°S–15°N	15°–35°N	35°–65°N	65°–90°N	15°S–15°N	15°–35°N	35°–65°N	65°–90°N
Cu	13	19	14	11	21	28	18	14
Sc	15	12	10	13	17	16	20	19
St	1	2	3	7	1	2	5	11
LI	29	33	27	31	39	46	43	44
Ac	9	11	18	22	13	14	14	21
As	13	11	13	17	8	7	13	17
Ns	3	4	5	5	1	2	5	7
MI	25	26	36	44	22	23	32	45
Ci	31	28	25	20	26	20	12	7
Cs	10	9	8	4	9	8	9	3
Cb	5	4	4	1	4	3	4	1
HI	46	41	37	25	39	31	25	11

Middle-level clouds have either one or two layers, but we assume that the total optical thickness of HL is less than that of ML, consistent with the decrease of cloud water contents with altitude. All LI clouds are single layer by definition. Table 4 shows the distribution of cloud amounts for the three standard ISCCP optical thickness categories separated by $\tau = 3.6$ and 23. To obtain a better match to the raobs layer cloud amounts, the high clouds are divided into four optical thickness ranges and the middle clouds into three ranges:

$$\mathrm{HI} = 1\mathrm{H}(\tau < 3.6) + \mathrm{HM}(3.6 < \tau < 9.4) + \mathrm{HML}(9.4 < \tau < 23) + \mathrm{Cb}(23 < \tau) \quad (8a)$$

and

$$\mathrm{MI} = 1\mathrm{M}(\tau < 1.3) + \mathrm{HL}(1.3 < \tau < 9.4) + \mathrm{ML}(9.4 < \tau). \quad (8b)$$

Table 3 shows (again asterisks indicate the best agreement with raobs) that the Model B results agree with the raobs about as well as Model A and better than random or maximum overlap. The key point is that Model B can be applied to individual scenes, whereas Model A (and Weare's 1999 results) can only be applied to monthly statistics.

Figures 1, 2, and 3 show the zonal-mean annual cycle of the normalized layer cloud amounts before and after these adjustments. The adjusted ISCCP low-level cloud amounts have been significantly increased in Models A and B, but they are still much lower than raobs except in the polar regions (Fig. 1). The revised ISCCP cloud amounts exhibit quantitatively similar seasonal variations as those of raobs except over subtropical oceans, where the ISCCP cloud amounts decrease in summer–autumn, and over polar land areas, where they exhibit too large a winter–summer difference. Middle-level cloud amounts in ISCCP Model A agree better with raobs than those of Model B at lower latitudes except over subtropical land areas where the ISCCP results show a larger seasonal variation with a maximum in autumn, whereas ISCCP Model B middle cloud amounts are in better agreement in midlatitudes (Fig. 2). Neither model improves the agreement between ISCCP and raobs middle-level clouds at higher latitudes in wintertime; the ISCCP amounts are persistently larger, exhibiting a larger seasonal cycle (maximum in winter) than those shown by raobs. The adjusted ISCCP high-level cloud amounts now exceed the unadjusted raobs amounts (by design) at lower latitudes by 10%–20%, consistent with expected raobs underestimates, but are still significantly less than the unadjusted raobs at higher latitudes, particularly over land (Fig. 3). The general land–ocean differences are in reasonable agreement for all cloud categories. Overall, Model A provides a better estimate of middle-level cloud amounts than Model B, but both still appear to underestimate low cloud amounts. Both models are an improvement over either random or maximum overlap results, however.

e. Discussion

Both Models A and B do about as well reconstructing the relative amount of low-level clouds, but still appear to underestimate low cloud cover, especially at lower latitudes, whereas maximum overlap overestimates the relative amount but comes closer to raobs. However, since raobs, itself, overestimates low-level cloud occurrence, especially at lower latitudes over the ocean, the maximum overlap results are not actually an improvement. In Table 5 we compare the absolute cloud fractions reported in the (independent) SOBS dataset with the original ISCCP areal cloud amounts and those obtained with Models A and B. Figure 1 compares the normalized cloud fractions from SOBS to Model A and B results. The comparison in Table 5

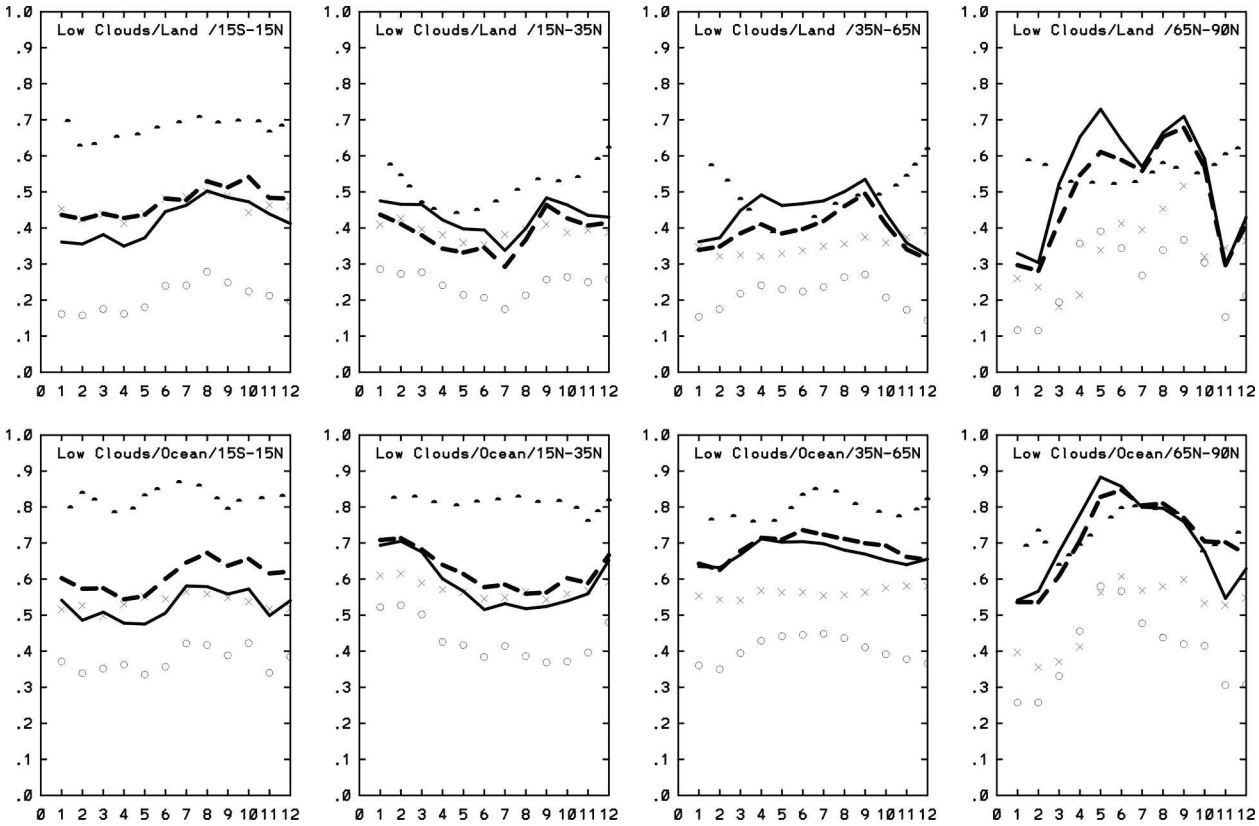

FIG. 1. Annual cycle of normalized low-level cloud amounts shown by the monthly Northern Hemispheric averages for (top) land and (bottom) ocean separately in four latitude zones. The original ISCCP values (open circles), the raobs frequency (closed circles), the SOBS cloud fraction (crosses), the adjusted ISCCP Model A values (thick dashed line), and the Model B values (thick solid line) are shown.

shows that the revised ISCCP low cloud fractions (both Model A and B) are actually in good agreement with SOBS at lower latitudes but appear to be too large by about 10%–20% at higher latitudes. Note, Tables 1 and 3 show that the low cloud amount from random overlap is somewhat similar to these two models and that maximum overlap would be an even larger overestimate than either Model A or B.

A quantitative comparison of our results to those from Weare (1999) is difficult because all we have from his paper are maps of cloud amount with relatively large contour intervals. The most interesting statistic he presents is the ratio of low-level cloud amount to total cloud amount (his Fig. 8). His maps show a nearly geographically uniform value for this quantity but with a distinct land–ocean difference. Over oceans this ratio increases from about 0.75 to about 0.95 from equator to pole; over land this ratio is about 0.75 with little indication of latitude dependence. Table 3 shows that the raobs ratios (these are normalized values) decrease with latitude from about 0.8 to about 0.7 over oceans and from about 0.7 to 0.6 over land. For Model B, this ratio increases with latitude from about 0.5 to 0.7 over oceans and from 0.4 to 0.5 over land. SOBS seems to confirm a decrease in low cloud amount with latitude over land. This disagreement of the latitude dependence will need to be resolved by the CloudSat/Cloud–Aerosol Lidar and Infrared Pathfinder Satellite Observation (CALIPSO) missions.

The apparent overestimate of adjusted ISCCP low cloud amounts in the polar regions compared with SOBS is systematic, but somewhat larger in summertime (Fig. 1). It is notable that the seasonal cycle of low clouds is mirrored by an opposite seasonal cycle of middle-level clouds that leads to a wintertime high bias of adjusted ISCCP middle-level cloud amounts relative to raobs (Fig. 2). This excess middle-level cloudiness in wintertime extends into midlatitudes as well. However, the total absolute ISCCP cloud amount in polar summertime is less than SOBS-based estimates, but is similar in wintertime (Curry et al. 1996; Rossow and Schiffer 1999). Comparisons of different satellite estimates appear to agree better on the amount of upper-level cloudiness (Jin et al. 1996; Stubenrauch et al.

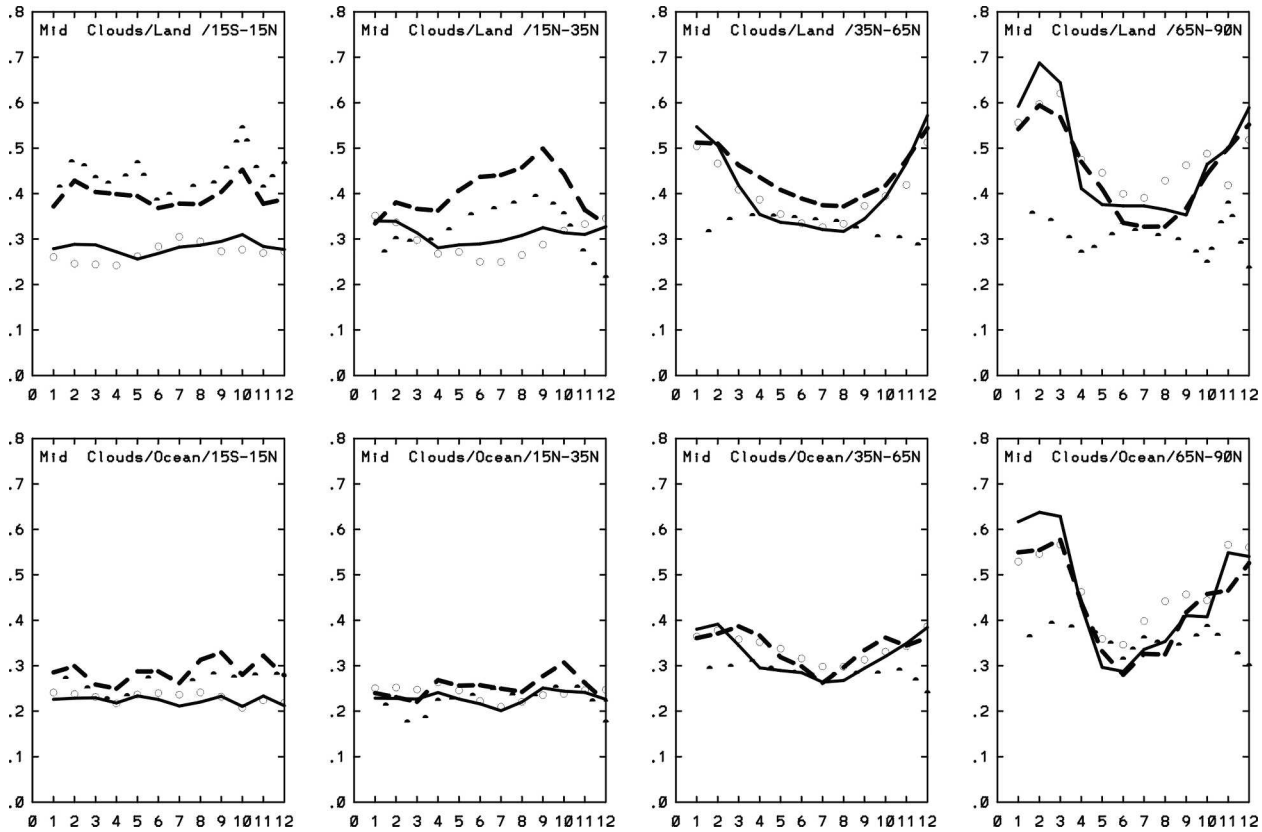

FIG. 2. Annual cycle of normalized middle-level cloud amounts shown by the monthly Northern Hemispheric averages for (top) land and (bottom) ocean separately in four latitude zones. The original ISCCP values (open circles), the raobs frequency of occurrence (closed circles), the adjusted ISCCP Model A values (thick dashed line), and the Model B values (thick solid line) are shown.

1999), whereas the ISCCP summertime underestimate appears to be associated with a preponderance of thin, low-level cloudiness that occurs during that season. Combining all these factors and remembering that the raobs probably overestimates the occurrence of ice phase clouds, we suggest that the ISCCP estimates of upper-level cloudiness are more reliable than those of raobs but that the apparent overestimate of low cloud amounts in the adjusted ISCCP results actually compensates, in part, for low clouds missed in the original ISCCP results. Model A had the advantage that it actually reduced the upper-level cloud amounts for raobs, while increasing the low-level cloud amounts. Model B accepts the ISCCP determination of upper-level clouds (these are not adjusted) and increases the lower-level clouds, maybe too much. For now, we have to accept these overestimates as the main limitation of this CVS reconstruction.

Another way to evaluate these results is to examine the average cloud-base pressure inferred from the ISCCP layer cloud amounts with and without the adjustments by Model B. Zhang et al. (1995) showed that the ISCCP results, combined with climatological cloud layer thicknesses, underestimated the monthly, zonal mean cloud-base pressures by 50–250 mb when assuming that all clouds are single layered. Zhang et al. (2004) show that adjusting the ISCCP CVS using Model B reduces this bias to < 100 mb except in the intertropical convergence zone (ITCZ) over land.

f. Summary

The results in Table 3 show that Models A and B are both generally superior to using the random or maximum overlap assumptions. Although Model B is only slightly better than Model A, it has the major advantages that the CVS is meteorologically dependent and the CVS assumptions can be applied to individual cases. In any case, neither model can be described as being perfect; these are crude statistical adjustments. A more thorough treatment is not justified because of the inherent uncertainties and sparseness of the raobs sampling. Chen et al. (2000b) show that different simple overlap schemes produced differences in the radiative heating rate profiles that are of the same order as the total effect produced by simply adding clouds to a particular layer. Thus, the agreement achieved here for

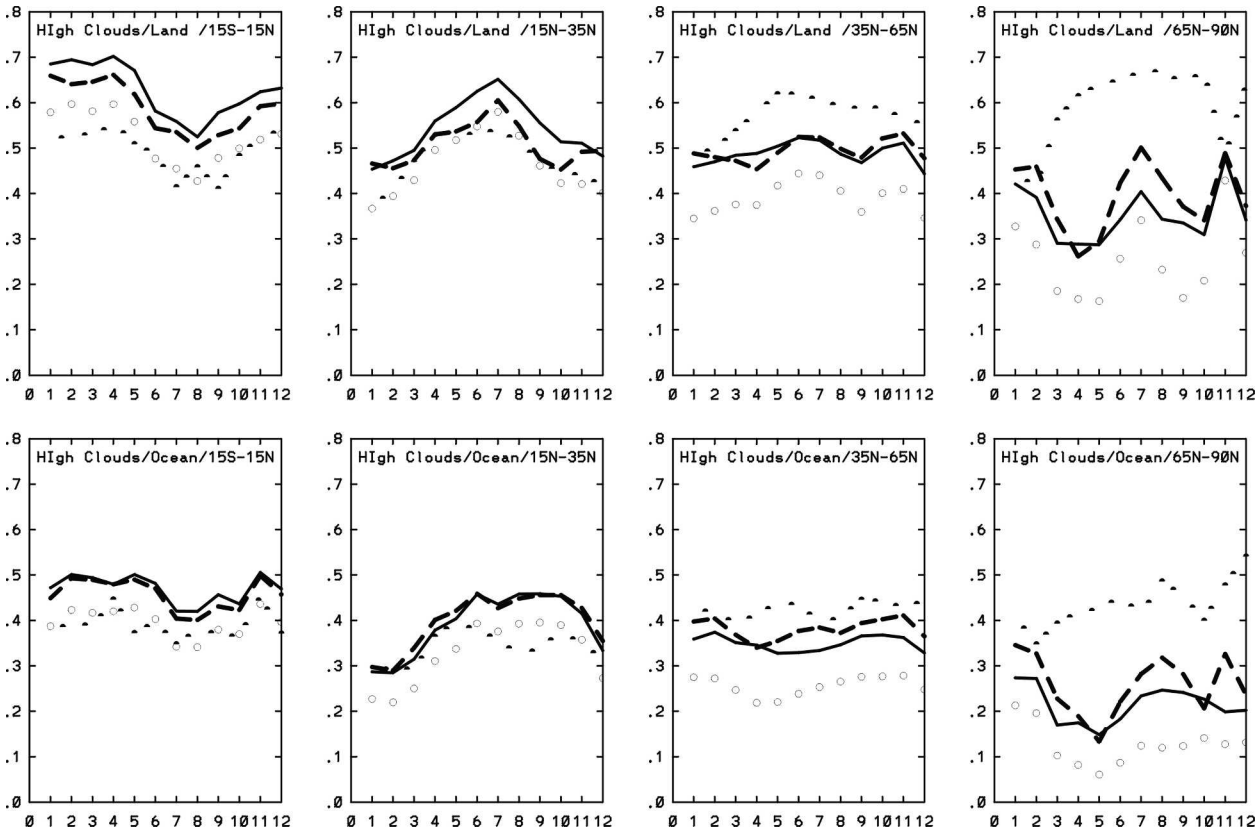

FIG. 3. Annual cycle of normalized high-level cloud amounts shown by the monthly Northern Hemispheric averages for (top) land and (bottom) ocean separately in four latitude zones. The original ISCCP values (open circles), the unadjusted raobs frequency of occurrence (closed circles), the adjusted ISCCP Model A values (thick dashed line), and the Model B values (thick solid line) are shown.

cloud layer amounts (within ± 5%–10%), as much as we are able to verify, is somewhat better than the 10%–20% differences tested by Chen et al., providing a useful reduction of the errors in radiative heating rate profiles. A successful CloudSat/CALIPSO mission will provide much better information about cloud vertical structure in the near future, allowing for more accurate determinations of the vertical profiles of radiative heating.

4. Cloud vertical structure

Figure 4 displays the zonal mean cloud fractions (the CVS) in each 50-mb layer of the atmosphere over land and ocean, averaged over January and July for 1990–92, that result from the Model B combination of raobs and the ISCCP D1 dataset (with some interpolation to extend the results to the nighttime and to fill missing observations; cf. Zhang et al. 2004). Notable global features are 1) high-level cloud amounts generally decrease from lower to higher latitudes, except for Antarctica in wintertime and midlatitude continents in summertime; 2) both middle-level and low-level cloud amounts increase from lower to higher latitudes (the latter consistent with surface observations over the oceans at least, cf. Table 5); 3) middle-level cloud amounts are generally less than both low-level and

TABLE 5. Comparison of original ISCCP (LI), Model A, and Model B absolute low cloud fractions with SOBS (LS).

	Land				Ocean			
Source	15°S–15°N	15°–35°N	35°–65°N	65°–90°N	15°S–15°N	15°–35°N	35°–65°N	65°–90°N
LS	29	20	21	24	32	32	42	39
LI	10	10	12	18	19	24	30	29
Model A	28	18	24	33	35	36	52	51
Model B	24	21	27	36	29	34	51	51

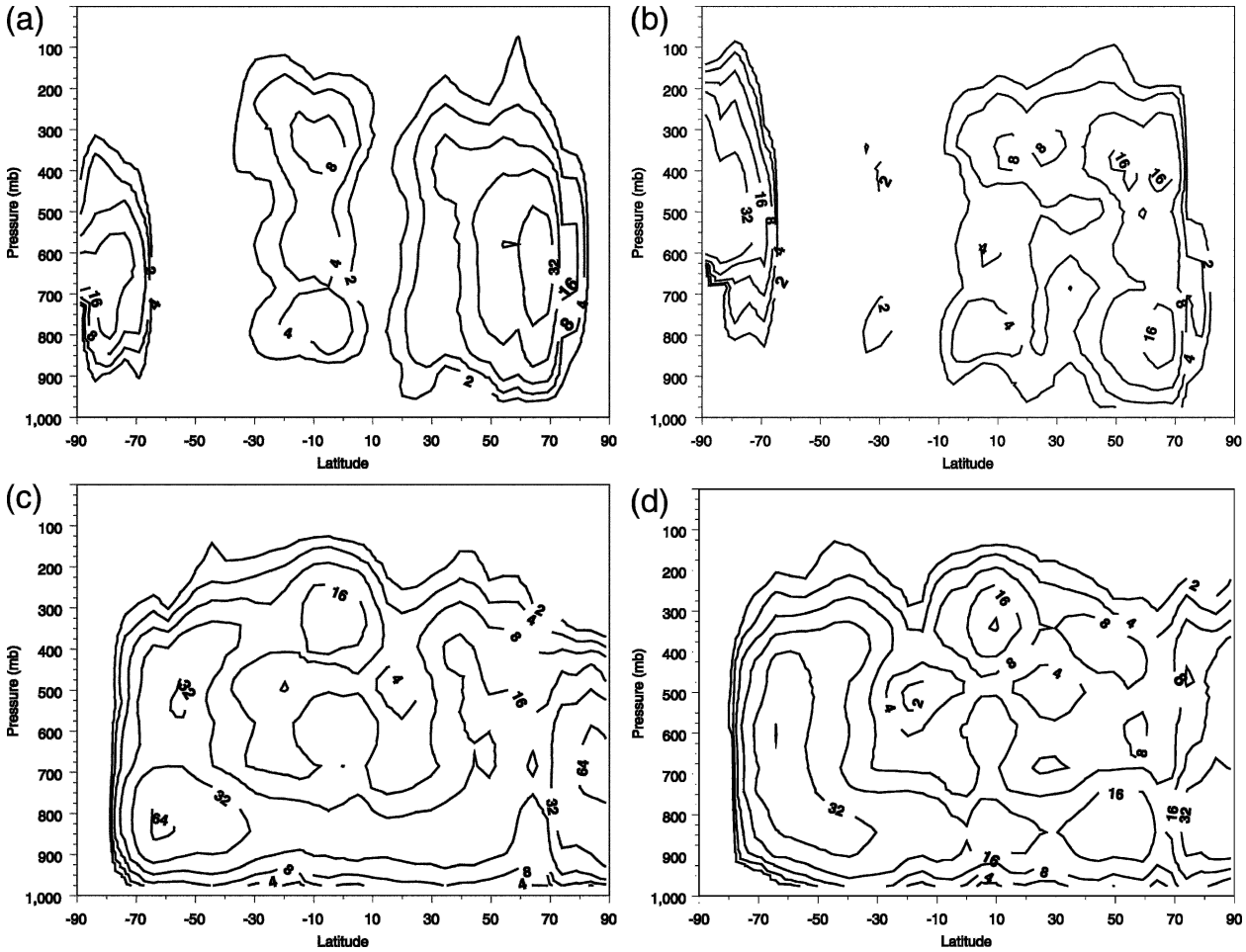

FIG. 4. Adjusted ISCCP Model B zonal, seasonal mean cloud vertical structure (cloud amounts in percent) for (a) land in Jan, (b) land in Jul, (c) ocean in Jan, and (d) ocean in Jul.

high-level cloud amounts, except in the polar regions; 4) high-level and low-level cloud amounts are generally larger over tropical oceans than over tropical land areas; 5) high-level cloud amounts are much larger in summertime over midlatitude land areas than over oceans at the same latitudes; and 6) low-level cloud amounts are much larger over subtropical and midlatitude oceans than over adjacent land areas.

When the ITCZ is over Southern Hemisphere land areas (January), it covers a broader latitude zone (30°S to the equator, southern Africa, and the Amazon Basin) than when it is in the Northern Hemisphere (July). Over the ocean the ITCZ is also narrower in July but in January it shows a hint of a double structure. The CVS of the tropical convective zone exhibits a characteristic triple-peak distribution; this is the same zone where the raobs climatology (Table 2) has the largest frequency of high–middle–low cloud, particularly over land areas, and where the ISCCP climatology (Table 4) has the largest frequency of high-level clouds with medium optical thicknesses, particularly over land areas (interpreted as convective anvil clouds with bases in the middle troposphere; cf. Machado and Rossow 1993; Luo and Rossow 2004). This triple structure is also consistent with the general association of cirrus with either altostratus/stratus and cumulus found by Warren et al. (1985; cf. Hahn et al. 2001) and recent results that have noted convective clouds topping out at three levels in the western Pacific (Johnson et al. 1999; cf. Jakob and Tselioudis 2003).

The subtropics are notable as a minimum of cloud fraction at all levels over land, but over oceans there is a local concentration of low-level clouds with little upper-level cloudiness. In the raobs climatology (Table 2), this is the zone with the largest amount of isolated low-level clouds and, in the ISCCP climatology (Table 4), this is the zone with the largest amount of low-level cloud as seen from above. The seasonal variations of

the Tropics and subtropics are generally produced by a latitudinal shifting of the convective and nonconvective zones; in the Northern Hemisphere summertime, the tropical CVS (triple peak) extends into the subtropics and lower midlatitudes at some longitudes. In general, the low-level clouds over oceans occur at a somewhat lower level than over land: Although this is partly a topographical effect (low-level clouds cannot occur over high topography, by definition), this is also a real difference, as shown by the SOBS climatology (Warren et al. 1985).

The midlatitude CVS exhibits a strong seasonal variation but with less shifting of latitude, especially in the Southern Hemisphere: the wintertime CVS is a single broad vertical distribution with a peak at middle levels (roughly 400–800 mb), whereas the summertime CVS is double peaked (reminiscent of the Tropics) with the upper-level peak at about the 400-mb level over land and about the 500-mb level over ocean. In Northern Hemisphere wintertime, the vertical extent of cloudiness is about the same over land and ocean but, in summertime, high-level clouds are more frequent and extend to somewhat higher levels over land than over oceans. Upper-level cloudiness is generally larger over the ocean in southern midlatitudes than in northern midlatitudes.

The Arctic (ice-covered ocean) shows summertime cloudiness extending to higher levels than in winter, but with a much stronger concentration of clouds at low levels in summertime than in wintertime. Antarctica (ice-covered land) exhibits an even larger seasonal variation from predominantly low- and middle-level clouds in summertime to a very extensive distribution of clouds to above the 100-mb level in wintertime (including some polar stratospheric clouds).

Figure 5 shows adaptations of two cartoons from Lau and Crane (1995) that portray the composite horizontal and vertical distribution of ISCCP cloud types in midlatitude cyclones: they have been changed to indicate how Model B changes the CVS. The characteristic "comma shape" of high, thick clouds is located between the low and high pressure center (Fig. 5a); the vertical cross section (Fig. 5b) shows that the optically thickest ISCCP clouds occur where the upward air motions are strongest. In this area, Model B assigns a combination of three-level clouds and extensive single-layer clouds (Cb) with bases in the boundary layer. As this "cold front" line of very thick clouds, which also corresponds to the heaviest precipitation (Lau and Crane 1997), approaches from the west, the sequence of ISCCP cloud types that appears is low-level, thin-to-medium thickness clouds, followed by a mix of low, middle, and high thin-to-medium thickness clouds, followed by optically thin high-level clouds, gradually thickening into the frontal clouds. That the ISCCP middle-level clouds in this sequence appear in between regions dominated by high- and low-level optically thin clouds suggests that these middle-level cloud are more likely a combination of high and low clouds misidentified by ISCCP as middle-level clouds. Model B makes this change from middle to high and low level. As the air motions change from downward to upward, the high-level clouds become optically thicker (Fig. 5b). Model B first assigns a high–middle CVS as the thickness increases, producing cloud bases at middle levels. Thus, as the cold front advances, Model B predicts the correct lowering of cloud bases until the onset of precipitation. This region

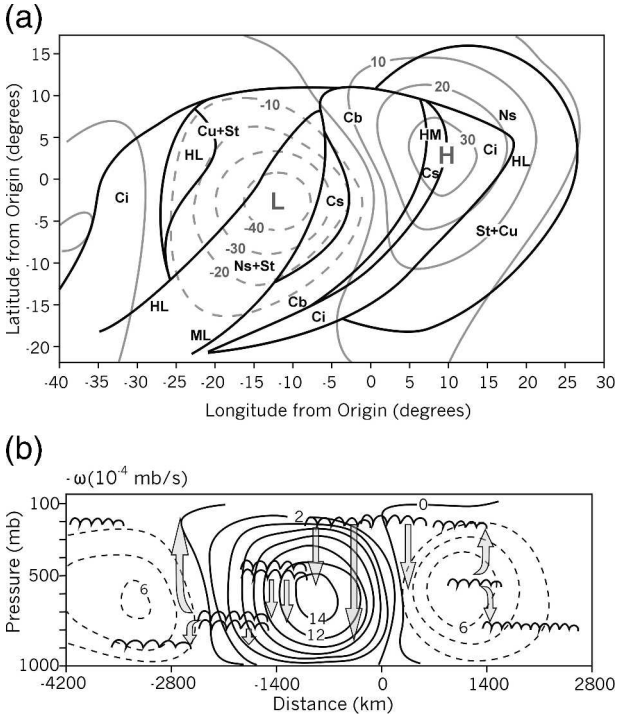

FIG. 5. A schematic of the composite structure of cloud types reported by Lau and Crane (1995) based on ISCCP for a midlatitude cyclone indicating the characteristic cloud vertical structure assigned by Model B. (a) The solid black lines indicate horizontal areas of similar ISCCP cloud types indicated by the mixed case symbols for the classical cloud types (e.g., St, Cu, etc.), and the gray solid and dashed lines show the surface pressure anomalies. In a few locations the capital letter symbols for various two-layer structures are indicated. (b) A vertical cross section showing the average vertical velocity (in intervals of 2×10^{-4} mb s^{-1}, positive upward indicated by solid contours) and the composite locations of cloud tops found by ISCCP (indicated by scalloped horizontal lines). The gray arrows indicate where cloud bases are moved downward, and, in some cases, cloud tops are moved upward, by the cloud vertical structure Model B. The classical depiction of the cloud-layer structure during a cold frontal passage corresponds well with these adjustments.

has the most noticeable difference between the satellite and surface reports (Lau and Crane 1997), with the former reporting high-level clouds and the latter reporting low-level clouds; Model B CVS adds more low-level clouds in this area. Behind the cold front, there is a trailing region of high-level medium-thickness clouds so that Model B predicts rising cloud bases. However, over the low pressure center there is a region of weakening updrafts and middle-level, optically thick clouds that is also associated with significant precipitation; Model B assigns a middle–low CVS to some of these clouds. This is consistent with the surface reports of significant low-level cloud in this area (Lau and Crane 1997). That this assignment makes sense is also suggested by the adjacent region exhibiting a mixture of middle-level and low-level optically thick clouds. The trailing edge of this mixed region (Fig. 5a) has progressively thinner clouds, so Model B changes from a middle–low to a high–low CVS, again consistent with the transition farther west to a mixture of low-level cloud types, especially to the northwest, and cirrus, especially to the west and southwest. The optically thicker low-level cloud to the northwest corresponds to surface reports of snowfall in wintertime cyclones (Lau and Crane 1997).

The results illustrated in Fig. 5 highlight the main implication of the relationships found among cloud types, their vertical structure, and the meteorology, namely, that the profiles of radiative and latent heating perturbations caused by clouds are correlated with variations of the atmospheric structure in these storm systems. For example, the increasing cloud tops and decreasing cloud bases associated with the strongest upward motions in a midlatitude cycle cause an increasing midatmosphere radiative heating that coincides with the heaviest precipitation, suggesting that the cloud effects on the diabatic heating of the atmosphere reinforce the strength of the circulation that forms them. This means that the effects of clouds on the atmospheric energy budget cannot be accurately determined using time–space averaged cloud and atmospheric properties as is generally done. Rather, compositing (Tselioudis et al. 2000) is necessary to capture the correlations of cloud and atmospheric properties in order to properly elucidate the effects that clouds have on the atmospheric circulation.

5. Final comments

The main purpose of this paper is to document the statistical model of CVS used for the reconstruction of radiative flux profiles using a variety of global datasets and a radiative transfer model (Zhang et al. 2004). Nevertheless, the CVS is interesting in its own right. This is reinforced by the statistical relationships that are found between the ISCCP-based cloud types and the raobs-based CVS that appear to reconstruct the global distribution of layer cloud amounts well enough that the radiative flux profiles may have useful accuracy (cf. Zhang et al. 2004). That such a simple set of assumptions appears to reconcile the different views of CVS rather well strengthens the association of meteorological situation with ISCCP cloud properties that has been found in a series of other recent studies (Machado and Rossow 1993; Lau and Crane 1995, 1997; Machado et al. 1998; Hahn et al. 2001; Tselioudis et al. 2000; Jakob and Tselioudis 2003). The resulting particular relations of CVS with meteorology are not new results (e.g., see drawing of frontal cloud cross sections in Byers 1937), as observations of cloud properties were the foundation of weather forecasting, but the availability of global satellite observations makes a much more precise, comprehensive, and general quantification of these relationships possible. In the next few years, with the addition of CloudSat (cloud profiling radar) and CALIPSO (cloud profiling lidar) to the constellation of weather and experimental satellites, there will be an unprecedented combination of instruments to describe the three-dimensional distribution of cloud properties and their synoptic variations. These properties can be linked with the meteorology using the several systematic weather analyses now produced by the weather services. Such an analysis is another use of these CVS results.

These results are not "final" conclusions because they are not direct measurements of the association of CVS with cloud types identified by their optical properties nor with specific meteorological situations. This model provides the most complete inference that we can construct from all of the partial information now available, but it lacks a specification of the vertical distribution of cloud water content and microphysical properties that is necessary to link meteorology through cloud structure to the precipitation process. The new combinations of satellite measurements may provide this advance (Stephens et al. 2002).

Acknowledgments. This work was supported by the NASA Pathfinder program (J. Dodge) and the Radiation Science program (H. Maring, formerly D. Anderson).

REFERENCES

Baum, B. A., B. A. Wielicki, P. Minnis, and S. C. Tsay, 1994: Multilevel cloud retrieval using multispectral HIRS and AVHRR

data: Nighttime oceanic analysis. *J. Geophys. Res.,* **99,** 5499–5514.

Byers, H. R., 1937: *Synoptic and Aeronautical Meteorology*. McGraw-Hill, 252 pp.

Chen, T., and W. B. Rossow, 2002: Determination of top-of-atmosphere longwave radiative fluxes: A comparison between two approaches using ScaRaB data. *J. Geophys. Res.,* **107,** 4070, doi:10.1029/2001JD000914.

——, ——, and Y.-C. Zhang, 2000a: Radiative effects of cloud-type variations. *J. Climate,* **13,** 264–286.

——, Y.-C. Zhang, and W. B. Rossow, 2000b: Sensitivity of radiative heating rate profiles to variations of cloud layer overlap. *J. Climate,* **13,** 2941–2959.

Chernykh, I. V., and R. E. Eskridge, 1996: Determination of cloud amount and level from radiosonde soundings. *J. Appl. Meteor.,* **35,** 1362–1369.

Curry, J. A., W. B. Rossow, D. Randall, and J. L. Schramm, 1996: Overview of Arctic cloud and radiation characteristics. *J. Climate,* **9,** 1731–1764.

Fu, R., A. D. Del Genio, and W. B. Rossow, 1990: Behavior of deep convective clouds in the tropical Pacific deduced from ISCCP radiances. *J. Climate,* **3,** 1128–1152.

Gierens, K., U. Schumann, M. Helten, H. Smit, and A. Marenco, 1999: A distribution law for relative humidity in the upper troposphere and lower stratosphere derived from three years of MOZAIC measurements. *Ann. Geophys.,* **17,** 1218–1226.

Hahn, C. J., S. G. Warren, J. London, R. M. Chervin, and R. L. Jenne, 1982: Atlas of simultaneous occurrence of definite cloud types over oceans. NCAR Tech. Note TN-201+STR, 29 pp.

——, ——, ——, ——, and ——, 1984: Atlas of simultaneous occurrence of definite cloud types over land. NCAR Tech. Note TN-241+STR, 42 pp.

——, ——, and ——, 1994: Climatological data for clouds over the globe from surface observations, 1982–1991: Total cloud edition. Carbon Dioxide Information Analysis Center, Oak Ridge National Laboratory Tech. Rep. NDP026A, 42 pp.

——, ——, and ——, 1996: Edited synoptic cloud reports from ships and land stations over the globe, 1982–1991. Carbon Dioxide Information Analysis Center, Oak Ridge National Laboratory Tech. Rep. NDP026B, 45 pp.

——, W. B. Rossow, and S. G. Warren, 2001: ISCCP cloud properties associated with standard cloud types identified in individual surface observations. *J. Climate,* **14,** 11–28.

Hogan, R. J., and A. J. Illingworth, 2000: Deriving cloud overlap statistics from radar. *Quart. J. Roy. Meteor. Soc.,* **126,** 2903–2909.

——, and ——, 2003: Parameterizing ice cloud inhomogeneity and the overlap of inhomogeneities using cloud radar data. *J. Atmos. Sci.,* **60,** 756–767.

Jakob, C., and G. Tselioudis, 2003: Objective identification of cloud regimes in the tropical western Pacific. *Geophys. Res. Lett.,* **30,** 2082, doi:10.1029/2003GL018367.

Jin, Y., and W. B. Rossow, 1997: Detection of cirrus overlapping low-level clouds. *J. Geophys. Res.,* **102,** 1727–1737.

——, ——, and D. P. Wylie, 1996: Comparison of the climatologies of high-level clouds from HIRS and ISCCP. *J. Climate,* **9,** 2850–2879.

Johnson, R. H., T. M. Rickenbach, S. A. Rutledge, P. E. Ciesielski, and W. H. Schubert, 1999: Trimodal characteristics of tropical convection. *J. Climate,* **12,** 2397–2418.

Kropfli, R. A., and Coauthors, 1995: Cloud physics studies with 8 mm wavelength radar. *Atmos. Res.,* **35,** 299–314.

Lau, N.-C., and M. W. Crane, 1995: A satellite view of the synoptic-scale organization of cloud properties in midlatitude and tropical circulation systems. *Mon. Wea. Rev.,* **123,** 1984–2006.

——, and ——, 1997: Comparing satellite and surface observations of cloud patterns in synoptic-scale circulation systems. *Mon. Wea. Rev.,* **125,** 3172–3189.

Liao, X., W. B. Rossow, and D. Rind, 1995a: Comparison between SAGE II and ISCCP high-level clouds, Part I: Global and zonal mean cloud amounts. *J. Geophys. Res.,* **100,** 1121–1135.

——, ——, and ——, 1995b: Comparison between SAGE II and ISCCP high-level clouds. Part II: Locating cloud tops. *J. Geophys. Res.,* **100,** 1137–1147.

Lin, B., B. A. Wielicki, P. Minnis, and W. B. Rossow, 1998: Estimation of water cloud properties from satellite microwave, infrared and visible measurements in oceanic environments. 1. Microwave brightness temperature simulations. *J. Geophys. Res.,* **103,** 3873–3886.

Luo, Z., and W. B. Rossow, 2004: Characterizing tropical cirrus life cycle, evolution, and interaction with upper-tropospheric water vapor using Lagrangian trajectory analysis of satellite observations. *J. Climate,* **17,** 4541–4563.

——, ——, T. Inoue, and C. J. Stubenrauch, 2002: Did the eruption of the Mt. Pinatubo volcano affect cirrus properties? *J. Climate,* **15,** 2806–2820.

Machado, L. A. T., and W. B. Rossow, 1993: Structural characteristics and radiative properties of tropical cloud clusters. *Mon. Wea. Rev.,* **121,** 3234–3260.

——, ——, R. L. Guedes, and A. W. Walker, 1998: Life cycle variations of mesoscale convective systems over the Americas. *Mon. Wea. Rev.,* **126,** 1630–1654.

Naud, C. M., J. P. Muller, and E. E. Clothiaux, 2003: Comparison between active sensor and radiosonde cloud boundaries over the ARM Southern Great Plains site. *J. Geophys. Res.,* **108,** 4140, doi:10.1029/2002JD002887.

Platt, C. M. R., and Coauthors, 1994: The Experimental Cloud Lidar Pilot Study (ECLIPS) for cloud-radiation research. *Bull. Amer. Meteor. Soc.,* **75,** 1635–1654.

Poore, K., J.-H. Wang, and W. B. Rossow, 1995: Cloud layer thicknesses from a combination of surface and upper air observations. *J. Climate,* **8,** 550–568.

Rind, D., and W. B. Rossow, 1984: The effects of physical processes on the Hadley circulation. *J. Atmos. Sci.,* **41,** 479–507.

Ross, R. J., and W. P. Elliott, 2001: Radiosonde-based Northern Hemisphere tropospheric water vapor trends. *J. Climate,* **14,** 1602–1612.

Rossow, W. B., and A. A. Lacis, 1990: Global, seasonal cloud variations from satellite radiance measurements. Part II: Cloud properties and radiative effects. *J. Climate,* **3,** 1204–1253.

——, and R. A. Schiffer, 1991: ISCCP cloud data products. *Bull. Amer. Meteor. Soc.,* **72,** 2–20.

——, and Y.-C. Zhang, 1995: Calculation of surface and top-of-atmosphere radiative fluxes from physical quantities based on ISCCP datasets. Part II: Validation and first results. *J. Geophys. Res.,* **100,** 1167–1197.

——, and R. A. Schiffer, 1999: Advances in understanding clouds from ISCCP. *Bull. Amer. Meteor. Soc.,* **80,** 2261–2287.

——, A. W. Walker, and L. C. Garder, 1993: Comparison of ISCCP and other cloud amounts. *J. Climate,* **6,** 2394–2418.

——, ——, D. Beuschel, and M. Roiter, 1996: International Satellite Cloud Climatology Project (ISCCP) documentation of

new cloud datasets. WMO Tech. Doc. 737, World Meteorological Organization, 115 pp.

Rozendaal, M., and W. B. Rossow, 2003: Characterizing some of the influences of the general circulation on subtropical marine boundary layer clouds. *J. Atmos. Sci.,* **60,** 711–728.

Sassen, K., 1991: The polarization lidar technique for cloud research: A review and current assessment. *Bull. Amer. Meteor. Soc.,* **72,** 1848–1866.

Seidel, D. J., and Coauthors, 2004: Uncertainty in signals of large-scale climate variations in radiosonde and satellite upper-air temperature datasets. *J. Climate,* **17,** 2225–2240.

Sheu, R.-S., J. Curry, and G. S. Liu, 1997: Vertical stratification of tropical cloud properties as determined from satellite. *J. Geophys. Res.,* **102,** 4231–4246.

Spichtinger, P., K. Gierens, and W. Read, 2003: The global distribution of ice-supersaturated regions as seen by the Microwave Limb Sounder. *Quart. J. Roy. Meteor. Soc.,* **129,** 3391–3410.

Stephens, G. L., and Coauthors, 2002: The CloudSat mission and the A-train: A new dimension of space-based observations of clouds and precipitation. *Bull. Amer. Meteor. Soc.,* **83,** 1771–1790.

Stubenrauch, C. J., W. B. Rossow, F. Cheruy, A. Chedin, and N. A. Scott, 1999: Clouds as seen by satellite sounders (3I) and imagers (ISCCP). Part I: Evaluation of cloud parameters. *J. Climate,* **12,** 2189–2213.

Tian, L., and J. A. Curry, 1989: Cloud overlap statistics. *J. Geophys. Res.,* **94,** 9925–9935.

Tselioudis, G., Y.-C. Zhang, and W. B. Rossow, 2000: Cloud and radiation variations associated with northern midlatitude low and high sea level pressure regimes. *J. Climate,* **13,** 312–327.

Uttal, T., E. E. Clothiaux, T. P. Ackerman, J. M. Intrieri, and W. L. Eberhard, 1995: Cloud boundary statistics during FIRE II. *J. Atmos. Sci.,* **52,** 4276–4284.

Wang, J., and W. B. Rossow, 1995: Determination of cloud vertical structure from upper air observations. *J. Appl. Meteor.,* **34,** 2243–2258.

——, and ——, 1998: Effects of cloud vertical structure on atmospheric circulation in the GISS GCM. *J. Climate,* **11,** 3010–3029.

——, ——, T. Uttal, and M. Rozendaal, 1999: Variability of cloud vertical structure during ASTEX from a combination of rawinsonde, radar, ceilometer, and satellite data. *Mon. Wea. Rev.,* **127,** 2484–2502.

——, ——, and Y.-C. Zhang, 2000: Cloud vertical structure and its variations from a 20-year global rawinsonde dataset. *J. Climate,* **13,** 3041–3056.

——, H. L. Cole, D. J. Carlson, E. R. Miller, K. Beierle, A. Paukkunen, and T. K. Laine, 2002: Corrections of humidity measurement errors from the Vaisala RS80 radiosonde—Application to TOGA COARE data. *J. Atmos. Oceanic Technol.,* **19,** 981–1002.

——, D. J. Carlson, D. B. Parsons, T. F. Hock, D. Lauritsen, H. L. Cole, K. Beierle, and E. Chamberlain, 2003: Performance of operational radiosonde humidity sensors in direct comparison with a chilled mirror dew-point hygrometer and its climate implications. *Geophys. Res. Lett.,* **30,** 1860, doi:10.1029/2003GL016985.

Wang, P.-H., P. Minnis, M. P. McCormick, G. S. Kent, and K. M. Skeens, 1996: A 6-year climatology of cloud occurrence frequency from Stratospheric Aerosol and Gas Experiment II observations (1985–1990). *J. Geophys. Res.,* **101,** 29 407–29 429.

Warren, S. G., C. J. Hahn, and J. London, 1985: Simultaneous occurrence of different cloud types. *J. Climate Appl. Meteor.,* **24,** 658–667.

——, ——, ——, R. M. Chervin, and R. L. Jenne, 1986: Global distribution of total cloud cover and cloud type amounts over land. NCAR Tech. Note TN-273+STR, 229 pp.

——, ——, ——, ——, and ——, 1988: Global distribution of total cloud cover and cloud type amounts over oceans. NCAR Tech. Note TN-317+STR, 212 pp.

Weare, B. C., 1999: Combined satellite- and surface-based observations of clouds. *J. Climate,* **12,** 897–913.

Wylie, D. P., and P.-H. Wang, 1997: Comparison of cloud frequency data from the High-Resolution Infrared Radiometer Sounder and the Stratospheric Aerosol and Gas Experiment II. *J. Geophys. Res.,* **102,** 29 893–29 900.

Zhang, Y.-C., W. B. Rossow, and A. A. Lacis, 1995: Calculation of surface and top-of-atmosphere radiative fluxes from physical quantities based on ISCCP datasets. Part I: Method and sensitivity to input data uncertainties. *J. Geophys. Res.,* **100,** 1149–1165.

——, ——, ——, V. Oinas, and M. I. Mishchenko, 2004: Calculation of radiative fluxes from the surface to top of atmosphere based on ISCCP and other global data sets: Refinements of the radiative transfer model and the input data. *J. Geophys. Res.,* **109,** D19105, doi:10.1029/2003JD004457.